Electronic Supplementary Material (ESI) for Lab on a Chip.

The biomolecular corona of gold nanoparticles in a controlled microfluidic environment

Luca Digiacomo,[1] Sara Palchetti,[1] Francesca Giulimondi,[1] Daniela Pozzi,[1] Riccardo Zenezini Chiozzi,[2] Anna Laura Capriotti,[3] Aldo Laganà,[3] Giulio Caracciolo[1]*

[1]*Department of Molecular Medicine, "Sapienza" University of Rome, Viale Regina Elena 291, 00161 Rome, Italy*

[2]*Biomolecular Mass Spectrometry and Proteomics, Bijvoet Center for Biomolecular Research and Utrecht Institute for Pharmaceutical Sciences, Utrecht University, Padualaan 8, 3584 CH Utrecht, The Netherlands*

[3]*Department of Chemistry, "Sapienza" University of Rome, P.le A. Moro 5, 00185 Rome, Italy*

*giulio.caracciolo@uniroma1.it

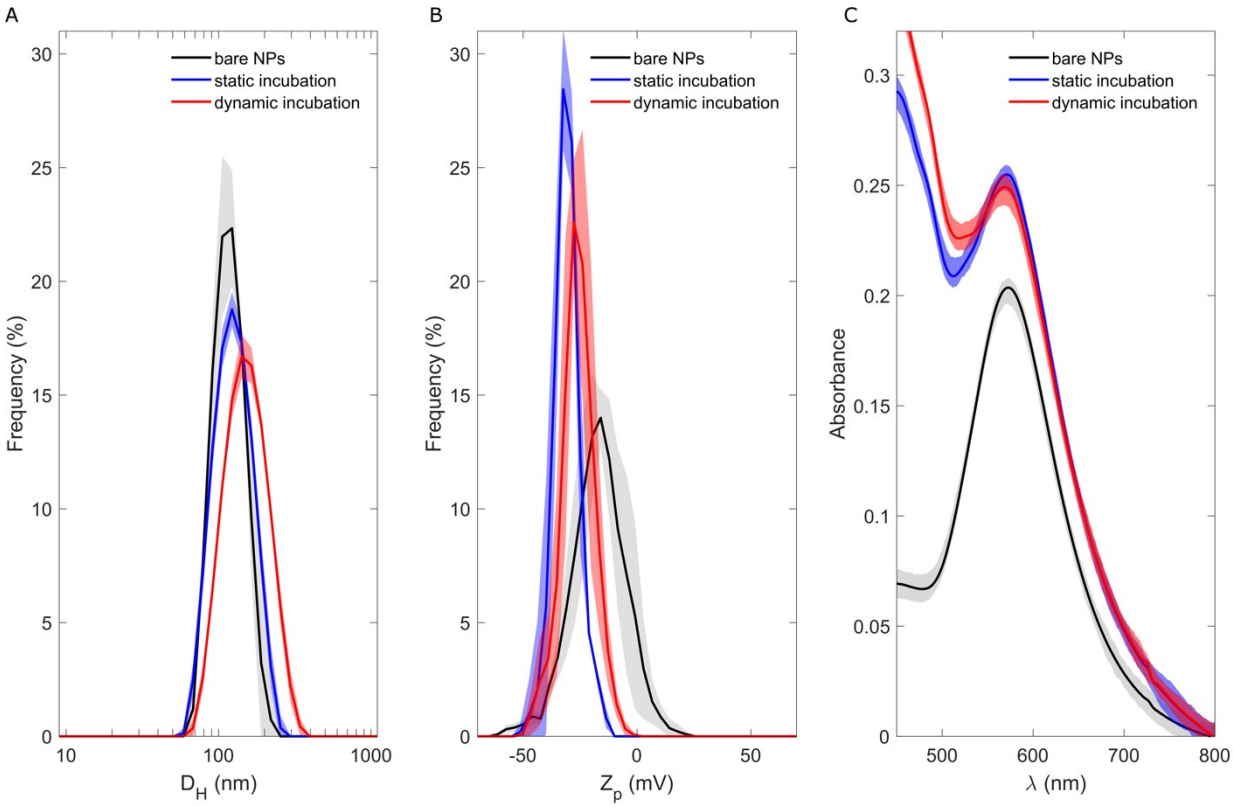

Fig. S1 (A) Size distributions by intensity, (B) Zeta potential distributions and (C) absorption spectra of bare gold nanoparticles (black) and gold nanoparticle-protein complexes upon static (blue) and dynamic (red) incubation with human plasma. Average curves ± standard deviations of three independent measurements are represented by solid lines within shaded areas.

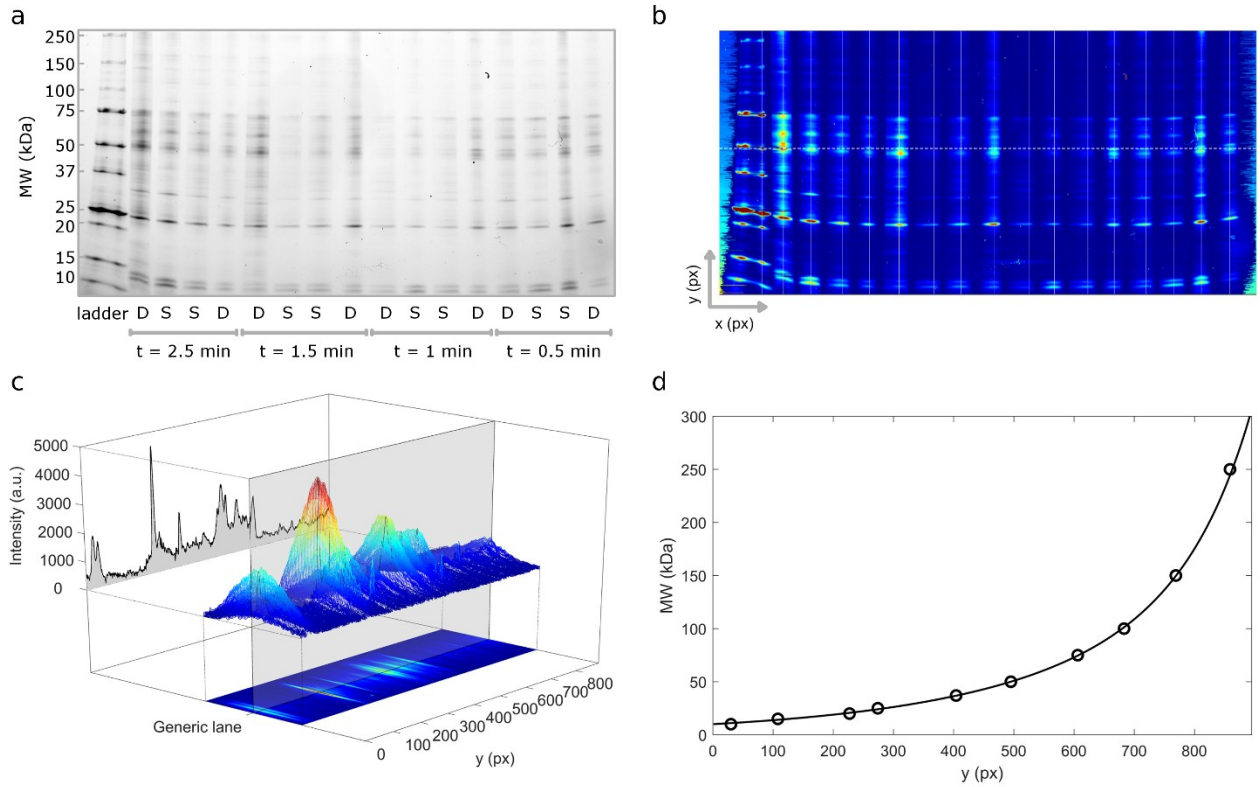

Fig. S2 Gel images were processed by custom Matlab (Mathworks) scripts to obtain the protein patterns associated to each sample. A representative gel image is shown in Fig. S2 (a), where the first lane represents a reference ladder and the remaining lanes correspond to the loaded samples (D:dynamic incubation; S: static incubation). A preliminary background removal was performed to prevent unwanted baselines affect the resulting curves. In detail, for each image, a rolling ball background subtraction was carried out row by row and the rolling ball radius was kept constant for all the processed images. Fig. S2 (b) shows a pseudocolor representation of a background-subtracted gel image. Left and right sides are residual regions, within which a clear trend of the original image intensity can be recognized. Thus, if $I(x,y)$ represents the sampled intensity of the original gel image, a processed image $I'(x,y)$ is obtained after the background removal procedure,

$I(x,y) \rightarrow I'(x,y)$

In other words, each gel image can be regarded as a functions (I') of two spatial variables (x and y), where the y-displacement is related to protein molecular weights and the intensity value to the protein amount. The projection (P) of this two-variable function over a plane orthogonal to the image is the resulting protein pattern of a generic lane (j) (Fig. S2 (c)):

$P_j(y) = I'(x_j,y)$

Finally, y-displacements can be converted to molecular weights (MW) by fitting the position of known proteins (ladder lane) to a non-linear equation (Fig. S2 (d)), as an instance:

$MW(y) = a_1 e^{b_1 y} + a_2 e^{b_2 y}$

Hence, for all the other lanes, the resulting one-dimensional profiles represent the molecular weight distributions of the corresponding samples.

$P_j(y) \rightarrow P_j(MW)$

All the distributions were finally normalized to 1.

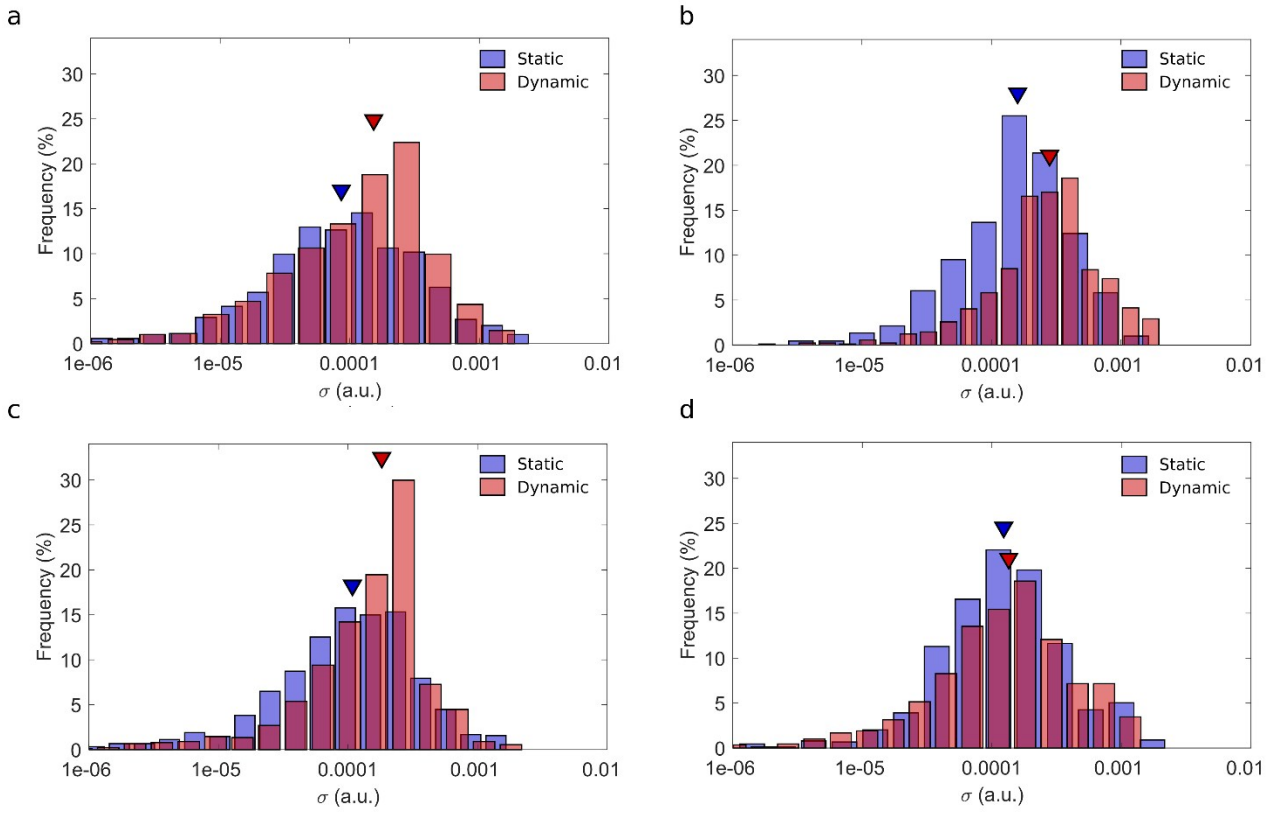

Fig. S3 Distributions of experimental errors (σ) at varying incubation times: 0,5-min (a), 1-min (b), 1,5-min (c), 2,5-min (d). Triangles indicate median of distributions. In detail, σ represents the standard deviation among the N replicates at a single point (x_k) of the MW axis.

$$\sigma = \sqrt{\sum_{i=1}^{N} \frac{(y_i(x_k) - \langle y(x_k) \rangle)^2}{N-1}}$$

Thus, for each of the eight conditions we obtain M values of σ, where M is the total number of discrete points along the MW axis.

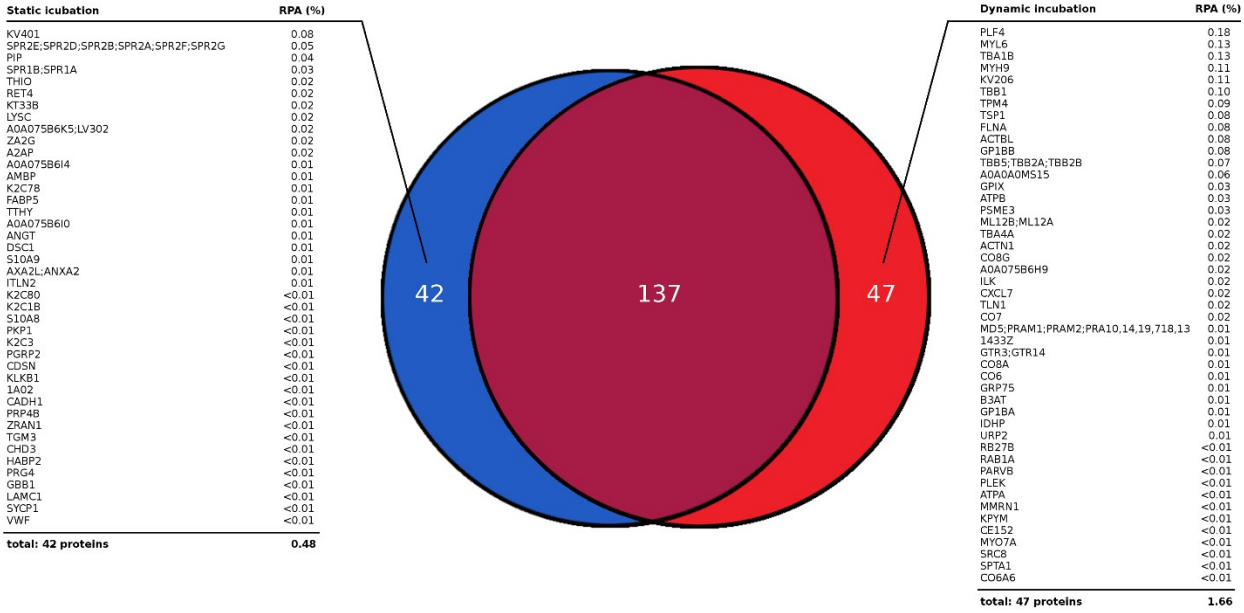

Static icubation	RPA (%)
KV401	0.08
SPR2E;SPR2D;SPR2B;SPR2A;SPR2F;SPR2G	0.05
PIP	0.04
SPR1B;SPR1A	0.03
THIO	0.02
RET4	0.02
KT33B	0.02
LYSC	0.02
A0A075B6K5;LV302	0.02
ZA2G	0.02
A2AP	0.02
A0A075B6I4	0.01
AMBP	0.01
K2C78	0.01
FABP5	0.01
TTHY	0.01
A0A075B6I0	0.01
ANGT	0.01
DSC1	0.01
S10A9	0.01
AXA2L;ANXA2	0.01
ITLN2	0.01
K2C80	<0.01
K2C1B	<0.01
S10A8	<0.01
PKP1	<0.01
K2C3	<0.01
PGRP2	<0.01
CDSN	<0.01
KLKB1	<0.01
1A02	<0.01
CADH1	<0.01
PRP4B	<0.01
ZRAN1	<0.01
TGM3	<0.01
CHD3	<0.01
HABP2	<0.01
PRG4	<0.01
GBB1	<0.01
LAMC1	<0.01
SYCP1	<0.01
VWF	<0.01
total: 42 proteins	**0.48**

Dynamic incubation	RPA (%)
PLF4	0.18
MYL6	0.13
TBA1B	0.13
MYH9	0.11
KV206	0.11
TBB1	0.10
TPM4	0.09
TSP1	0.08
FLNA	0.08
ACTBL	0.08
GP1BB	0.08
TBB5;TBB2A;TBB2B	0.07
A0A0A0MS15	0.06
GPIX	0.03
ATPB	0.03
PSME3	0.03
ML12B;ML12A	0.02
TBA4A	0.02
ACTN1	0.02
CO8G	0.02
A0A075B6H9	0.02
ILK	0.02
CXCL7	0.02
TLN1	0.02
CO7	0.02
MD5;PRAM1;PRAM2;PRA10,14,19,718,13	0.01
1433Z	0.01
GTR3;GTR14	0.01
CO8A	0.01
CO6	0.01
GRP75	0.01
B3AT	0.01
GP1BA	0.01
IDHP	0.01
URP2	0.01
RB27B	<0.01
RAB1A	<0.01
PARVB	<0.01
PLEK	<0.01
ATPA	<0.01
MMRN1	<0.01
KPYM	<0.01
CE152	<0.01
MYO7A	<0.01
SRC8	<0.01
SPTA1	<0.01
CO6A6	<0.01
total: 47 proteins	**1.66**

Fig. S4 Venn diagram of the proteins identified by mass spectrometry. 137 proteins (60.6%) are in common; 42 plasma proteins (18.6%) are only present in the static corona, while 47 plasma proteins (20.8%) exclusively enrich the dynamic corona.

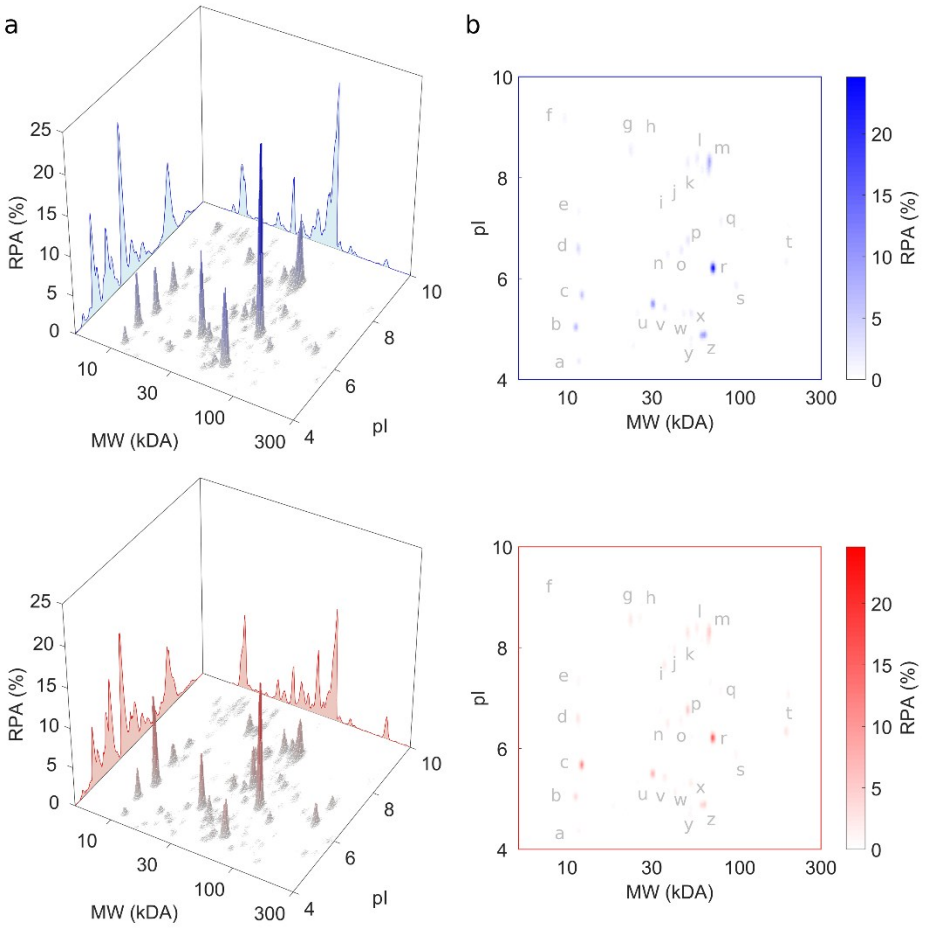

	protein	RPA static	RPA dynamic
a	APOC2	1.1%	0.5%
b	APOC3	4.7%	2.9%
c	IGKC	4.5%	10.6%
d	APOA2	2.9%	2.3%
e	LAC6	0.7%	1.0%
f	APOC1	1.1%	0.1%
g	IGLL5	2.0%	3.1%
	LAC1	2.0%	3.1%
h	C1QC	0.1%	1.0%
i	IGHG2	0.3%	2.0%
j	IGHG3	0.4%	1.5%
k	IGHG1	1.8%	3.1%
l	FIBB	1.9%	2.0%
m	K2C1	9.2%	6.2%
	K22E	3.6%	2.3%
n	IGHA1	1.0%	1.7%
o	HPT	1.6%	1.0%
p	IGHM	2.2%	5.3%
q	TRFE	1.2%	0.7%
r	ALBU	21.3%	15.8%
s	FIBA	1.1%	1.0%
t	CO3	0.9%	2.1%
u	APOA1	7.9%	6.2%
v	APOE	1.8%	1.5%
w	ACTB	<0.1%	1.0%
	A1AT	0.8%	0.4%
x	FIBG	1.3%	1.4%
y	K1C14	0.6%	0.4%
z	K1C9	5.6%	3.4%
	K1C10	4.5%	1.9%

Fig. S5 (a) Distributions of relative protein abundance (RPA) of identified proteins, based on their molecular weights (MW) and isolectric points (pI). The coronas were formed by incubation under static (blue) and dynamic (red) conditions. (b) Projection of protein distributions in the MW vs. pI plane. (c) Lists of plasma proteins corresponding to the spots identified in panel B. Color intensity is proportional to RPA.

Table S1 Hydrodynamic diameter (D_H), polydispersity index (PdI), zeta potential and absorption maximum of bare gold nanoparticles (NP) and NP-protein complexes. NP-protein complexes were formed exposing bare gold NPs to human plasma for 0,5 min at 37°C. Dynamic incubation was realized using a remote-controlled microfluidic device, while static incubation was used as a reference.

	Bare Nanoparticles	Nanoparticle-protein complexes	
		Static	Dynamic
D_H (nm)	120.0 ± 5.2	128.6 ± 3.5	148.5 ± 2.3
PdI	0.153 ± 0.029	0.199 ± 0.009	0.164 ± 0.015
Zeta-potential (mV)	-21.2 ± 0.9	-30.9 ± 0.7	-26.1 ± 1.1
Absorbance peak (nm)	573 ± 3	571 ± 4	569 ± 5

Table S2 Quantitative estimation of experimental uncertainties associated to protein patterns reported in Fig. 2 panels B-E. Experimental uncertainties are expressed in terms of cumulative linear deviation Δ and cumulative standard deviation Σ. The i-th protein pattern (y_i) is a function of molecular weight (x) that is sampled along a discrete axis of M points. Δ is evaluated as

$$\Delta = \sum_{k=1}^{M} \delta_k = \sum_{k=1}^{M} \left(\sum_{i=1}^{N} \frac{|y_i(x_k) - \langle y(x_k) \rangle|}{N-1} \right)$$

Where N is the number of replicates and the average operation is carried out among the replicates at a single point (x_k) on the MW axis. Similarly

$$\Sigma = \sum_{k=1}^{M} \sigma_k = \sum_{k=1}^{M} \sqrt{\left[\sum_{i=1}^{N} \frac{(y_i(x_k) - \langle y(x_k) \rangle)^2}{N-1} \right]}$$

	Δ		Σ	
time (min)	static	dynamic	static	dynamic
0,5	0,240	0,275	0,169	0,194
1	0,282	0,489	0,199	0,346
1,5	0,226	0,280	0,160	0,198
2,5	0,259	0,288	0,183	0,204

Table S3 Relative protein abundance of proteins identified in the coronas of 100 nm gold nanoparticles following 1-min exposure to human plasma under microfluidic and static environment. Results are reported as mean values (MV) of three independent experiments +/- SD.

	Accession number	MW (kDa)	pI	Microfluidic MV	Microfluidic SD	Static MV	Static SD
1	ALBU_HUMAN	69,366	6,211	15,831%	0,592%	21,263%	0,476%
2	IGKC_HUMAN	11,765	5,677	10,644%	0,693%	4,485%	0,318%
3	K2C1_HUMAN	66,038	8,331	6,224%	0,516%	9,221%	0,611%
4	APOA1_HUMAN	30,777	5,499	6,157%	0,129%	7,900%	0,125%
5	IGHM_HUMAN	49,439	6,766	5,332%	0,138%	2,244%	0,164%
6	K1C9_HUMAN	62,064	4,889	3,344%	0,197%	5,558%	0,280%
7	IGLL5_HUMAN	22,83	8,5505	3,125%	0,049%	2,018%	0,044%
8	IGHG1_HUMAN	49,328	8,302	3,106%	0,067%	1,828%	0,041%
9	APOC3_HUMAN	10,852	5,041	2,868%	0,072%	4,672%	0,196%
10	CO3_HUMAN	187,15	6,338	2,605%	0,111%	0,912%	0,004%
11	K22E_HUMAN	65,432	8,17	2,314%	0,107%	3,650%	0,028%
12	APOA2_HUMAN	11,175	6,605	2,292%	0,053%	2,918%	0,039%
13	IGHG2_HUMAN	35,9	7,658	2,021%	0,100%	0,268%	0,051%
14	FIBB_HUMAN	55,928	8,39	1,965%	0,070%	1,910%	0,096%
15	K1C10_HUMAN	59,51	4,876	1,948%	0,368%	4,450%	0,059%
16	IGHA1_HUMAN	37,654	6,491	1,676%	0,326%	1,061%	0,027%
17	APOB_HUMAN	515,6	7,044	1,562%	0,106%	2,065%	0,043%
18	APOE_HUMAN	36,154	5,423	1,516%	0,080%	1,753%	0,257%
19	IGHG3_HUMAN	41,287	7,951	1,489%	0,092%	0,398%	0,016%
20	FIBG_HUMAN	51,511	5,321	1,354%	0,075%	1,339%	0,038%
21	CO4A_HUMAN	192,78	7,073	1,226%	0,147%	0,362%	0,033%
22	FIBA_HUMAN	94,972	5,868	1,070%	0,056%	1,147%	0,037%
23	C1QC_HUMAN	25,773	8,58	1,046%	0,042%	0,133%	0,052%
24	HPT_HUMAN	45,205	6,561	1,039%	0,056%	1,593%	0,188%
25	ACTB_HUMAN	41,736	5,143	1,011%	0,176%	0,032%	0,003%
26	LAC6_HUMAN	11,265	7,337	0,975%	0,455%	0,734%	0,022%
27	C4BPA_HUMAN	67,033	7,307	0,720%	0,160%	0,169%	0,005%
28	TRFE_HUMAN	77,063	7,132	0,684%	0,049%	1,164%	0,032%
29	K2C6C_HUMAN	60,024	8,17	0,580%	0,027%	0,989%	0,008%
30	APOH_HUMAN	38,298	8,024	0,576%	0,041%	0,228%	0,005%
31	APOA_HUMAN	501,31	5,766	0,556%	0,024%	0,719%	0,038%
32	C1QB_HUMAN	26,721	8,873	0,538%	0,006%	0,158%	0,002%
33	APOC2_HUMAN	11,284	4,368	0,522%	0,199%	1,121%	0,157%
34	C1QA_HUMAN	26,016	9,458	0,496%	0,004%	0,064%	0,001%
35	IGJ_HUMAN	18,098	4,863	0,480%	0,011%	0,173%	0,014%
36	CLUS_HUMAN	52,494	6,211	0,462%	0,006%	0,227%	0,019%
37	DCD_HUMAN	11,284	6,517	0,459%	0,038%	0,503%	0,177%
38	CD5L_HUMAN	38,087	5,143	0,451%	0,024%	0,155%	0,006%
39	FCN2_HUMAN	34,001	6,766	0,438%	0,080%	0,242%	0,042%
40	CRP_HUMAN	25,038	5,321	0,401%	0,040%	0,655%	0,056%
41	A1AT_HUMAN	46,736	5,308	0,401%	0,049%	0,815%	0,065%
42	K1C16_HUMAN	51,267	4,685	0,398%	0,028%	0,463%	0,034%
43	K1C14_HUMAN	51,621	4,813	0,343%	0,066%	0,626%	0,043%
44	SAA4_HUMAN	14,746	9,385	0,310%	0,037%	0,288%	0,052%
45	FCN3_HUMAN	32,903	6,664	0,262%	0,010%	0,004%	0,003%
46	APOD_HUMAN	21,275	4,8	0,243%	0,039%	0,241%	0,051%
47	A0A0C4DH25_HU	12,557	6,851	0,221%	0,059%	0,095%	0,007%
48	ITIH4_HUMAN	103,36	6,971	0,211%	0,022%	0,457%	0,013%
49	HBB_HUMAN	15,998	7,322	0,206%	0,012%	0,164%	0,017%
50	ITLN1_HUMAN	34,961	5,893	0,204%	0,020%	0,175%	0,017%
51	A0A0B4J1V1_HUI	12,943	9,1945	0,196%	0,050%	0,141%	0,008%
52	PROP_HUMAN	51,276	7,922	0,193%	0,027%	0,018%	0,005%
53	PLF4_HUMAN	10,845	8,785	0,183%	0,037%	0,000%	0,000%
54	HPTR_HUMAN	39,029	7,102	0,178%	0,028%	0,109%	0,013%
55	KRT86_HUMAN	53,5	5,251	0,168%	0,033%	0,201%	0,019%
56	A1AG1_HUMAN	23,511	4,66	0,166%	0,023%	0,522%	0,035%
57	K2C5_HUMAN	62,378	7,907	0,166%	0,033%	0,360%	0,005%
58	A0A0B4J1X5_HUI	12,839	8,5725	0,163%	0,108%	0,107%	0,093%
59	IGHG4_HUMAN	35,94	7,41	0,156%	0,046%	0,042%	0,018%
60	K1H1_HUMAN	47,237	4,533	0,152%	0,014%	0,216%	0,012%
61	APOC1_HUMAN	9,3318	9,18	0,149%	0,042%	1,093%	0,302%
62	HBA_HUMAN	15,257	9,092	0,148%	0,023%	0,248%	0,014%
63	VTDB_HUMAN	52,917	5,207	0,130%	0,004%	0,113%	0,009%
64	MYL6_HUMAN	16,93	4,291	0,126%	0,025%	0,000%	0,000%
65	TBA1B_HUMAN	50,151	4,698	0,125%	0,016%	0,000%	0,000%
66	C1S_HUMAN	76,684	4,584	0,125%	0,006%	0,048%	0,004%
67	A0A0C4DH41_HU	13,815	8,536	0,125%	0,084%	0,015%	0,001%
68	C1R_HUMAN	80,118	6,148	0,124%	0,009%	0,044%	0,002%
69	MYH9_HUMAN	226,53	5,283	0,113%	0,006%	0,000%	0,000%
70	KV206_HUMAN	13,185	9,531	0,107%	0,096%	0,000%	0,000%
71	TBB1_HUMAN	50,326	4,825	0,098%	0,020%	0,000%	0,000%
72	TPM4_HUMAN	28,521	4,355	0,094%	0,043%	0,000%	0,000%
73	A2MG_HUMAN	163,29	6,427	0,091%	0,011%	0,145%	0,002%
74	ACTA_HUMAN	42,051	5,054	0,089%	0,009%	0,006%	0,000%
75	TSP1_HUMAN	129,38	4,507	0,080%	0,002%	0,000%	0,000%

	Accession number	MW (kDa)	pI	Microfluidic MV	Microfluidic SD	Static MV	Static SD
76	FLNA_HUMAN	280,74	5,957	0,080%	0,014%	0,000%	0,000%
77	ACTBL_HUMAN	42,003	5,283	0,079%	0,137%	0,000%	0,000%
78	GP1BB_HUMAN	21,717	9,37	0,076%	0,002%	0,000%	0,000%
79	CO4B_HUMAN	192,75	7,278	0,072%	0,003%	0,014%	0,005%
80	PON1_HUMAN	39,731	4,889	0,069%	0,010%	0,076%	0,005%
81	TBB5_HUMAN;	49,67	4,52	0,069%	0,015%	0,000%	0,000%
82	VTNC_HUMAN	54,305	5,537	0,069%	0,001%	0,082%	0,015%
83	CFAH_HUMAN	139,09	6,59	0,067%	0,009%	0,054%	0,002%
84	FETUA_HUMAN	39,34	5,525	0,066%	0,023%	0,125%	0,007%
85	APOA4_HUMAN	45,398	5,041	0,063%	0,007%	0,156%	0,003%
86	HV303_HUMAN	12,947	9,165	0,061%	0,006%	0,022%	0,002%
87	CO9_HUMAN	63,173	5,27	0,060%	0,016%	0,003%	0,001%
88	A0A0A0MS15_HU	13,056	8,814	0,057%	0,004%	0,000%	0,000%
89	ITA2B_HUMAN	113,38	5,029	0,056%	0,010%	0,002%	0,000%
90	ITB3_HUMAN	87,057	4,851	0,056%	0,009%	0,002%	0,001%
91	PLMN_HUMAN	90,568	7,249	0,054%	0,009%	0,013%	0,005%
92	A0A0C4DH31_HU	12,82	9,465	0,052%	0,004%	0,016%	0,002%
93	HEMO_HUMAN	51,676	7,015	0,052%	0,023%	0,133%	0,017%
94	KNG1_HUMAN	71,957	6,81	0,049%	0,001%	0,102%	0,019%
95	ITIH2_HUMAN	106,46	6,854	0,047%	0,005%	0,052%	0,005%
96	APOL1_HUMAN	43,974	5,55	0,041%	0,012%	0,034%	0,007%
97	KRA23_HUMAN;	13,48	7,878	0,036%	0,009%	0,033%	0,011%
98	LAC7_HUMAN	11,253	8,478	0,033%	0,028%	0,010%	0,000%
99	LV102_HUMAN	12,283	9,121	0,032%	0,004%	0,022%	0,001%
100	HORN_HUMAN	282,39	10,248	0,031%	0,003%	0,050%	0,003%
101	C4BPB_HUMAN	28,357	4,8	0,030%	0,008%	0,003%	0,003%
102	APOC4_HUMAN	14,553	9,136	0,029%	0,014%	0,103%	0,006%
103	GPIX_HUMAN	19,046	6,326	0,029%	0,008%	0,000%	0,000%
104	MASP1_HUMAN	79,246	5,181	0,029%	0,004%	0,012%	0,001%
105	KRT85_HUMAN	55,802	6,491	0,027%	0,015%	0,044%	0,010%
106	ATPB_HUMAN	56,559	5,067	0,027%	0,008%	0,000%	0,000%
107	K1C17_HUMAN	48,105	4,673	0,027%	0,019%	0,095%	0,008%
108	CALL5_HUMAN	15,892	4,05	0,026%	0,001%	0,036%	0,007%
109	PSME3_HUMAN	29,506	5,753	0,025%	0,002%	0,000%	0,000%
110	ML12B_HUMAN	19,794	4,425	0,025%	0,002%	0,000%	0,000%
111	AACT_HUMAN	47,65	5,194	0,024%	0,003%	0,061%	0,007%
112	HRG_HUMAN	59,578	7,527	0,024%	0,003%	0,043%	0,002%
113	SAMP_HUMAN	25,387	6,517	0,024%	0,002%	0,011%	0,000%
114	TBA4A_HUMAN	49,924	4,698	0,023%	0,005%	0,000%	0,000%
115	ACTN1_HUMAN	103,06	5,08	0,023%	0,006%	0,000%	0,000%
116	PROS_HUMAN	75,122	5,372	0,023%	0,008%	0,002%	0,002%
117	LBP_HUMAN	53,383	6,678	0,022%	0,006%	0,029%	0,005%
118	CO8G_HUMAN	22,277	8,478	0,020%	0,003%	0,000%	0,000%
119	CO5_HUMAN	188,3	6,491	0,019%	0,000%	0,001%	0,000%
120	GELS_HUMAN	85,696	6,186	0,018%	0,008%	0,018%	0,001%
121	STOM_HUMAN	31,73	8,068	0,018%	0,002%	0,001%	0,002%
122	A0A075B6H9_HU	12,773	6,491	0,018%	0,016%	0,000%	0,000%
123	ILK_HUMAN	51,419	8,185	0,018%	0,003%	0,000%	0,000%
124	A1AG2_HUMAN	23,602	4,762	0,017%	0,005%	0,063%	0,015%
125	KRT34_HUMAN	49,411	4,724	0,017%	0,001%	0,027%	0,007%
126	CXCL7_HUMAN	13,894	9,063	0,017%	0,015%	0,000%	0,000%
127	FINC_HUMAN	262,62	5,448	0,017%	0,001%	0,029%	0,000%
128	TLN1_HUMAN	269,76	5,931	0,016%	0,003%	0,000%	0,000%
129	CO7_HUMAN	93,517	6,44	0,016%	0,006%	0,000%	0,000%
130	LV301_HUMAN	12,042	6,504	0,015%	0,002%	0,015%	0,001%
131	A0A0G2JMD5_HU	55,091	8,375	0,014%	0,001%	0,000%	0,000%
132	K2C71_HUMAN	57,865	7,263	0,014%	0,002%	0,020%	0,007%
133	1433Z_HUMAN	27,745	4,431	0,013%	0,016%	0,000%	0,000%
134	K2C6A_HUMAN	60,044	8,17	0,013%	0,023%	0,004%	0,000%
135	GTR3_HUMAN	53,924	7,5705	0,012%	0,001%	0,000%	0,000%
136	A0A0B4J2H0_HUI	12,992	8,9165	0,012%	0,010%	0,009%	0,007%
137	A0A087WSX0_HU	13,394	8,0315	0,011%	0,000%	0,009%	0,001%
138	CO8A_HUMAN	65,163	6,415	0,011%	0,003%	0,000%	0,000%
139	APOM_HUMAN	21,253	5,919	0,010%	0,004%	0,059%	0,028%
140	CO6_HUMAN	104,79	6,737	0,010%	0,004%	0,000%	0,000%
141	CD9_HUMAN	25,416	7,19	0,010%	0,005%	0,001%	0,002%
142	KRA31_HUMAN	10,539	6,389	0,0092%	0,0160%	0,0189%	0,0006%
143	CERU_HUMAN	122,2	5,499	0,0085%	0,0039%	0,0311%	0,0005%
144	CFAB_HUMAN	85,532	7,073	0,0076%	0,0026%	0,0197%	0,0026%
145	G3P_HUMAN	36,053	8,726	0,0075%	0,0020%	0,0128%	0,0051%
146	A1BG_HUMAN	54,253	5,715	0,0072%	0,0028%	0,0296%	0,0081%
147	PLAK_HUMAN	81,744	6,046	0,0070%	0,0040%	0,0476%	0,0107%
148	FILA2_HUMAN	248,07	8,346	0,0069%	0,0006%	0,0198%	0,0034%
149	GRP75_HUMAN	73,68	6,008	0,0068%	0,0003%	0,0000%	0,0000%
150	B3AT_HUMAN	101,79	4,838	0,0063%	0,0002%	0,0000%	0,0000%

	Accession number	MW (kDa)	pI	Microfluidic MV	Microfluidic SD	Static MV	Static SD
151	1B58_HUMAN	40,337	6,249	0,0060%	0,0003%	0,0025%	0,0001%
152	HEP2_HUMAN	57,07	6,898	0,0060%	0,0003%	0,0046%	0,0013%
153	SBSN_HUMAN	60,54	7,015	0,0056%	0,0001%	0,0103%	0,0007%
154	GP1BA_HUMAN	71,539	6,237	0,0056%	0,0028%	0,0000%	0,0000%
155	IDHP_HUMAN	50,909	8,946	0,0052%	0,0046%	0,0000%	0,0000%
156	URP2_HUMAN	75,952	6,985	0,0051%	0,0002%	0,0000%	0,0000%
157	S10A7_HUMAN	11,305	7,176	0,0050%	0,0087%	0,0139%	0,0055%
158	RB27B_HUMAN	24,608	5,13	0,0049%	0,0086%	0,0000%	0,0000%
159	THRB_HUMAN	70,036	5,703	0,0048%	0,0028%	0,0379%	0,0117%
160	FHR1_HUMAN	37,65	7,424	0,0048%	0,0083%	0,0246%	0,0003%
161	K1C19_HUMAN	44,091	4,787	0,0043%	0,0038%	0,0029%	0,0025%
162	APOF_HUMAN	35,399	5,359	0,0042%	0,0036%	0,0077%	0,0001%
163	RAB1A_HUMAN	22,677	5,995	0,0041%	0,0072%	0,0000%	0,0000%
164	PARVB_HUMAN	41,714	6,722	0,0036%	0,0032%	0,0000%	0,0000%
165	DSG1_HUMAN	113,75	4,66	0,0031%	0,0001%	0,0260%	0,0025%
166	DMD_HUMAN	426,74	5,69	0,0028%	0,0025%	0,0001%	0,0001%
167	ITIH1_HUMAN	101,39	6,781	0,0024%	0,0002%	0,0200%	0,0017%
168	DESP_HUMAN	331,77	6,781	0,0020%	0,0012%	0,0197%	0,0010%
169	PLEK_HUMAN	40,124	8,448	0,0019%	0,0033%	0,0000%	0,0000%
170	ANT3_HUMAN	52,602	6,678	0,0019%	0,0032%	0,0256%	0,0057%
171	ATPA_HUMAN	59,75	9,56	0,0018%	0,0031%	0,0000%	0,0000%
172	CFAI_HUMAN	65,75	7,527	0,0018%	0,0015%	0,0011%	0,0009%
173	FA5_HUMAN	251,7	5,944	0,0017%	0,0012%	0,0065%	0,0001%
174	IC1_HUMAN	55,154	6,517	0,0015%	0,0026%	0,0229%	0,0009%
175	KPRP_HUMAN	64,135	8,287	0,0015%	0,0001%	0,0348%	0,0165%
176	MMRN1_HUMAN	138,11	8,009	0,0015%	0,0026%	0,0000%	0,0000%
177	KPYM_HUMAN	57,936	7,936	0,0011%	0,0020%	0,0000%	0,0000%
178	CE152_HUMAN	195,62	5,321	0,0011%	0,0001%	0,0000%	0,0000%
179	MYO7A_HUMAN	254,39	8,756	0,0011%	0,0000%	0,0000%	0,0000%
180	DYHC1_HUMAN	532,4	6,338	0,0005%	0,0001%	0,0004%	0,0003%
181	FILA_HUMAN	435,16	9,604	0,0005%	0,0007%	0,0006%	0,0002%
182	SRC8_HUMAN	61,585	5,041	0,0001%	0,0002%	0,0000%	0,0000%
183	SPTA1_HUMAN	280,01	4,685	0,0001%	0,0001%	0,0000%	0,0000%
184	CO6A6_HUMAN	247,17	6,868	0,0001%	0,0001%	0,0000%	0,0000%
185	A2AP_HUMAN	54,565	6,237	0,0000%	0,0000%	0,0152%	0,0036%
186	KV401_HUMAN	13,38	4,851	0,0000%	0,0000%	0,0817%	0,0167%
187	A0A075B6I4_HUN	12,395	8,244	0,0000%	0,0000%	0,0150%	0,0004%
188	A0A075B6K5_HU	12,332	6,1115	0,0000%	0,0000%	0,0198%	0,0018%
189	A0A075B6I0_HUN	12,814	4,139	0,0000%	0,0000%	0,0105%	0,0093%
190	AMBP_HUMAN	38,999	6,148	0,0000%	0,0000%	0,0135%	0,0038%
191	KT33B_HUMAN	46,213	4,495	0,0000%	0,0000%	0,0227%	0,0047%
192	K2C1B_HUMAN	61,802	5,779	0,0000%	0,0000%	0,0032%	0,0029%
193	K2C3_HUMAN	64,503	6,402	0,0000%	0,0000%	0,0021%	0,0020%
194	K2C78_HUMAN	56,964	5,83	0,0000%	0,0000%	0,0128%	0,0038%
195	K2C80_HUMAN	50,525	5,359	0,0000%	0,0000%	0,0041%	0,0008%
196	ANGT_HUMAN	53,154	6,275	0,0000%	0,0000%	0,0096%	0,0025%
197	AXA2L_HUMAN	38,604	7,4245	0,0000%	0,0000%	0,0063%	0,0017%
198	CADH1_HUMAN	97,455	4,329	0,0000%	0,0000%	0,0013%	0,0012%
199	CHD3_HUMAN	226,59	7,307	0,0000%	0,0000%	0,0009%	0,0001%
200	CDSN_HUMAN	51,522	8,419	0,0000%	0,0000%	0,0019%	0,0002%
201	SPR1B_HUMAN	9,8774	8,595	0,0000%	0,0000%	0,0258%	0,0016%
202	DSC1_HUMAN	99,986	5,08	0,0000%	0,0000%	0,0071%	0,0038%
203	FABP5_HUMAN	15,164	7,059	0,0000%	0,0000%	0,0125%	0,0007%
204	GBB1_HUMAN	37,377	5,855	0,0000%	0,0000%	0,0003%	0,0005%
205	1A02_HUMAN	40,921	7	0,0000%	0,0000%	0,0017%	0,0020%
206	HABP2_HUMAN	62,671	6,532	0,0000%	0,0000%	0,0008%	0,0015%
207	ITLN2_HUMAN	36,211	8,346	0,0000%	0,0000%	0,0051%	0,0044%
208	LAMC1_HUMAN	177,6	4,749	0,0000%	0,0000%	0,0003%	0,0004%
209	LYSC_HUMAN	16,537	9,355	0,0000%	0,0000%	0,0210%	0,0020%
210	PGRP2_HUMAN	62,216	7,585	0,0000%	0,0000%	0,0020%	0,0017%
211	PKP1_HUMAN	82,86	9,399	0,0000%	0,0000%	0,0027%	0,0002%
212	KLKB1_HUMAN	71,369	8,258	0,0000%	0,0000%	0,0017%	0,0005%
213	PIP_HUMAN	16,572	8,185	0,0000%	0,0000%	0,0442%	0,0057%
214	S10A8_HUMAN	10,834	7,073	0,0000%	0,0000%	0,0029%	0,0051%
215	S10A9_HUMAN	13,242	6,071	0,0000%	0,0000%	0,0064%	0,0110%
216	TGM3_HUMAN	76,631	5,601	0,0000%	0,0000%	0,0011%	0,0001%
217	PRG4_HUMAN	151,06	10,16	0,0000%	0,0000%	0,0005%	0,0004%
218	RET4_HUMAN	23,01	5,855	0,0000%	0,0000%	0,0227%	0,0101%
219	PRP4B_HUMAN	116,99	10,965	0,0000%	0,0000%	0,0012%	0,0000%
220	SPR2E_HUMAN	7,9653	8,4045	0,0000%	0,0000%	0,0462%	0,0138%
221	SYCP1_HUMAN	114,19	5,728	0,0000%	0,0000%	0,0002%	0,0003%
222	THIO_HUMAN	11,737	4,546	0,0000%	0,0000%	0,0234%	0,0078%
223	TTHY_HUMAN	15,887	5,575	0,0000%	0,0000%	0,0120%	0,0121%
224	ZRAN1_HUMAN	80,966	5,397	0,0000%	0,0000%	0,0011%	0,0020%
225	VWF_HUMAN	309,26	5,156	0,0000%	0,0000%	0,0001%	0,0002%
226	ZA2G_HUMAN	34,258	5,919	0,0000%	0,0000%	0,0156%	0,0022%